Corrosion of 304 Stainless Steel Exposed To Nitric Acid - Chloride Environments

D.G. Kolman, D.K. Ford, D.P. Butt, and T.O. Nelson

Materials Corrosion and Environmental Effects Laboratory
Los Alamos National Laboratory
Los Alamos, NM 87545

Abstract

In an effort to examine the combined effect of HNO_3, NaCl, and temperature on the general corrosion behavior of 304 stainless steel (SS), electrochemical studies were performed. It was found that the corrosion response of 304 SS was bifurcated: materials were either continuously passive following immersion or spontaneously passivated following a period of active dissolution. Active dissolution was autocatalytic, with the corrosion rate increasing exponentially with time and potential. The period of active corrosion terminated following spontaneous passivation, resulting in a corrosion rate decrease of up to 5 orders of magnitude. The length of the active corrosion period was strongly dependent on the solution volume to surface area ratio. This finding, coupled with other results, suggested that spontaneous passivation arises solely from solution chemistry as opposed to changes in surface oxide composition. Increasing NaCl concentrations promoted pitting, active dissolution upon initial immersion, a smaller potential range for passivity, longer active corrosion periods, larger active anodic charge densities preceding spontaneous passivation, and larger corrosion current and peak current densities. In contrast, intermediate HNO_3 concentrations promoted active dissolution, with continuous passivity noted at HNO_3 concentration extremes. During active corrosion, increased HNO_3 concentrations increased the anodic charge density, corrosion current density, and peak current density. The time required for spontaneous passivation was greatest at intermediate HNO_3 concentrations. Susceptibility to pitting was also greatest at intermediate HNO_3 concentrations. That is, the pit initiation and repassivation potentials decreased with increasing HNO_3 until the HNO_3 concentration exceeded a critical concentration beyond which susceptibility to pitting was entirely eliminated. Increasing solution temperature increased the susceptibility to both pitting and active dissolution.

Introduction

The processing of actinide salts in nitric acid (HNO_3) process streams plays an important role in high-level radioactive waste reduction and long-term storage of radioactive material. Container materials for HNO_3 process streams, such as pipes and holding vessels, are typically composed of AISI 304 stainless steel (SS). However, the corrosion resistance of 304 SS exposed to HNO_3/halide environments has been questioned.

In general, the corrosion behavior of 304 SS has been very well documented.[1,2,3] The recent literature alone is replete with studies of general and localized corrosion of 304 SS exposed to HNO_3 solutions[4,5,6,7,8,9] or to sodium chloride (NaCl) solutions.[10,11,12,13,14,15] However, little work incorporating the corrosion of 304 SS exposed to solutions containing both HNO_3 and NaCl has been published.

No single reported work to date has comprehensively examined the general corrosion behavior of 304 SS in the 0.01 M to 10 M HNO_3 range in the presence of NaCl. A variety of researchers have performed weight loss measurements in only one or a few different HNO_3/HF[16,17] or HNO_3/Cl^- [18,19,20,21] environments. Moreover, publication of potentiodynamic polarization curves in HNO_3/NaCl environments has been scant. Matantsev[22] produced potentiostatic polarization curves for a 17 Cr - 10 Ni - 0.5 Ti steel that appeared to indicate that increasing NaCl concentration resulted in increased passive current densities during exposure to approximately 1 M HNO_3. The curves, unfortunately, are composed of few data points and thus results are somewhat speculative. Gorodnichii and Rozenblyum[23] examined the corrosion behavior of an 18 Cr - 10 Ni - 0.7 Ti steel and found that increased NaCl concentrations promoted a passive-to-active transition. Additionally, the corrosion behavior was mapped as a function of NO_3^- and NaCl concentration for pH levels of 0, 0.5, and 1. The methodology used to generate these maps is unclear. It was found that the material could be active, passive, active/passive, or exhibit pitting depending on pH and NO_3^- concentrations. Petit *et al.* also mapped the corrosion behavior of 304 SS as a function of HNO_3 and NaCl concentrations[24]. They inferred regions of stress corrosion cracking, passivity, activity, and pitting/intergranular attack from scanning electron microscopy investigations that followed 120 hours of immersion in boiling solutions at various stress states. The method for delineation of the individual regions is unclear as pitting was noted in each region. However, their results indicated no pitting below 0.5 M NaCl in HNO_3 concentrations ranging from 0.1 to 5 M.

A study by Mirolyubov *et al.*[25] is perhaps the most comprehensive to date, although only a small range of HNO_3 concentration (1 M to 5 M) was examined. The authors noted that the

concentration of chloride required to activate 18 Cr - 9 Ni - 0.5 Ti steel increased with increasing temperature, HNO_3 concentration, and wt% Cr in the metal; and decreased with increasing wt% Ni, and corrosion product concentration. During active corrosion, increasing the HNO_3 concentration increased the corrosion rate. However, increasing the HNO_3 concentration beyond a certain point resulted in passivity. Thus, a maximum in corrosion rate was observed at intermediate HNO_3 concentrations. Mirolyubov *et al.* also found that there was a critical time required for spontaneous passivation of SS exposed to certain combinations of HNO_3 and NaCl. This was termed self-passivation because the material was found to spontaneously passivate while freely corroding in the absence of external polarization. The self-passivation time decreased with increasing HNO_3 concentration, temperature, wt% Cr, wt% Mo, wt% Ti, wt% Fe, and NO_2^- concentration, and increased with increasing NaCl concentration and solution volume to surface area (V:A) ratio. The self-passivation was attributed to the autocatalytic nature of HNO_3 reduction, which has also been proposed by others.[26,27] However, no evidence of autocatalytic corrosion (i.e., increasing corrosion rate with time preceding self-passivation) was presented. Tomashov, using an austenitic SS, suggested that chloride additions reduce the open circuit potential (OCP) by promoting anodic reactions and retarding cathodic reactions.[28] Inhibition of the cathodic reaction was hypothesized to result from Cl^- adsorption on the surface that prevented HNO_3 reduction to HNO_2.

The literature is also replete with studies examining the elevated temperature behavior of austenitic stainless steels exposed to either chloride or nitrate anions. The corrosion rate of 304 SS has been shown to increase with both temperature and HNO_3 concentration in elevated temperature solutions.[25,29] Also, it has been well documented that the pit initiation potential drops linearly with temperature in chloride solutions.[2] However, the elevated temperature corrosion behavior of 304 SS in solutions containing the combination of HNO_3 and NaCl has not been well documented. Matantsev showed, via weight loss studies, that increasing the chloride concentration and temperature increased the corrosion rate in 6.5% HNO_3.[22] Also via weight loss studies, Ciriscioli *et al.* found that the corrosion rate increased linearly with temperature in 5% HNO_3 + 20% $MgCl_2$, 5% HNO_3 + 30% $MgCl_2$, and 60% HNO_3 + 4% $MgCl_2$.[19] Additionally, weight loss tests on 304L SS exposed to HNO_3/HF solutions suggested that increasing HF concentration and temperature increased the corrosion rate. HNO_3 inhibited or accelerated corrosion, depending upon temperature and HF concentration.[17] Also, Al cations, added as $Al(NO_3)_3$, complexed the fluoride, resulting in a decrease in weight loss.[16,17] In none of these studies was the surface state examined using electrochemical measurements to discern the anodic and/or cathodic kinetics as a function of time and solution component concentration.

The localized corrosion behavior of 304 SS exposed to NO_3^-/Cl^- solutions has been better documented. Leckie and Uhlig[30] described the critical chloride concentration for pitting of 18 Cr - 9 Ni steel in $NaNO_3$ / NaCl solutions as $\log (Cl^-) = 1.88 \log (NO_3^-) + 1.18$, where (Cl^-) and (NO_3^-) represent the estimated activities of chloride and nitrate anions, respectively. They also showed, by means of potentiostatic polarization curves, that the pitting potential in 0.1 M $NaNO_3$ solutions decreased with increasing chloride level. Through weight loss measurements, Uhlig and Gilman[31] (using 19 Cr - 9 Ni steel) reported a slightly different relationship for $NaNO_3/FeCl_3$ solutions: $\log (Cl^-) = 1.92 \log (NO_3^-) + 1.34$. Matsuda and Uhlig[32] (using Fe - 0.023 C) inferred pitting susceptibility from weight loss measurements for a wide variety of $NaNO_2$/NaCl solutions. Greene and Fontana[33], using 304 SS, reported that nitrate ions effectively prevented pit initiation in chloride solutions but accelerated pit growth when the HNO_3 was added after pit initiation. Schwenk[34] observed that the critical Cl^- concentration required for pitting increased with increasing $NaNO_3$ for 18 Cr - 10 Ni steel.

In summary, individual tests using different combinations of HNO_3, NaCl, temperature, and material have been performed to date. The majority of these tests have only examined weight loss or surface state (by means of microscopy) without monitoring the electrochemical behavior of the system. The motivation for this study arises from the fact that between published studies: 1) different alloy compositions have been used; 2) various cations have been incorporated (e.g., $NaNO_3$ vs. HNO_3, NaCl vs. $FeCl_3$); 3) different testing periods have been used; and 4) different V:A ratios have been used. All of the preceding variations have been shown to affect results. Therefore, unification of data from the literature into a comprehensive understanding of corrosion susceptibility is nearly impossible. This is especially true in light of the fact that corrosion has been hypothesized to be autocatalytic[25], rendering comparisons between studies with differing test periods and V:A ratios difficult. In fact, testing periods and V:A ratios are not presented in many of the studies. The differences between the various studies are exacerbated by the fact that nitrates are powerful passivating agents and chlorides are powerful depassivating agents. Thus, nitrates and chlorides have strongly opposite effects, the sum of which may be altered by changing variables such as alloy composition and microstructure, solution composition, and test procedures.

The objective of this study was to accurately document the general corrosion behavior of stainless steel using modern electrochemical techniques, including potentiodynamic scans and OCP measurements, especially between 0.01 M and 1 M HNO_3 where little work has been performed. In particular, the effects of HNO_3 concentration (0.041 M - 12 M), NaCl concentration (0.01 M - 3 M), temperature (room temperature to boiling), V:A ratio, and time of exposure on the corrosion

behavior of 304 SS were of interest. A second objective of this work was to confirm the autocatalytic nature of general corrosion in HNO_3/NaCl environments that others have proposed. A third objective was to delineate the limitations of weight loss testing in HNO_3/NaCl solutions.

Experimental Procedure

Materials

The compositions of the alloys used in this study varied slightly within alloy types but fell within published specifications[35]. In order to avoid crevicing, flag-shaped working electrodes were exposed to solution without mounting. The 304 SS flag is a one piece electrode comprising two regions, the main body and a electrical lead. The electrical lead is a long thin portion which connects the rectangular main body to the electrometer outside of the cell. The main body comprises almost all of the area exposed to solution. Thus, the geometry mimics a flag pole (lead) and flag (main body). This geometry minimizes water-line effects since the water-line intersects the lead which has a much smaller area. Differential oxygenation effects at the waterline were further mitigated by coating the lead area at the waterline with an electrically insulating, noncrevicing compound (GLPT insulating varnish). Working electrode areas were 15 cm^2, except where noted. Specimens were polished to 800 grit finish followed by ultrasonic cleaning in a mixed hydrocarbon solution (100 ethanol : 1 methanol : 1 ethyl acetate : 1 methyl isobutyl ketone).

Environments

All solutions were prepared with distilled water and reagent grade chemicals. All solutions were actively aerated (oxygen concentration = 6.4 ppm). Air was introduced to solution by fine porosity gas dispersion tubes with flow rates of approximately 90 cm^3/min (0.2 scfh). Solution resistances, as measured by replicate electrochemical impedance spectroscopy tests, varied from 0.43 Ω (4 M HNO_3 + 1 M NaCl) to 5.8 Ω (0.04 M HNO_3), depending on solution composition. Solution volumes for immersion tests and potentiodynamic polarization tests were 400 ml and 500 ml, respectively, except where noted. These volumes yield V:A ratios of 26.7 cm^3/cm^2 and 33.3 cm^3/cm^2, respectively, for 15 cm^2 specimen areas. All tests below 100°C were performed at an altitude of 7200 ft. above sea level. This altitude yielded boiling points of HNO_3/NaCl solutions between 86°C and 94°C (+/- 1°C). Some tests were reproduced at sea level to examine the corrosion behavior at increased boiling temperatures (101°C - 113°C). The form of corrosion

behavior observed (active, passive, or pitting) was similar at altitude and sea level, although the kinetics were slightly altered.

Electrochemical Testing

Electrochemical measurements were performed with several different commercially available potentiostats under software control. Potentiodynamic scan rates of 0.05 mV/s were utilized. Samples were immersed in solution for 4 hours at open circuit (OC) preceding polarization, except where noted. Electrochemical cells were composed of platinized Nb counter electrodes and either a saturated calomel electrode (SCE) or Ag/AgCl electrode as a reference electrode. All potentials are referenced to the SCE at 25°C.[36] Linear polarization resistance measurements incorporated potentiodynamic scans from -10 mV_{OCP} to +10 mV_{OCP} at a scan rate of 0.05 mV / s. Elevated temperature tests incorporated a condenser to prevent solution loss.

Results and Discussion

Effects of Time

As an initial survey, 304 SS samples were immersed in actively aerated test solutions for one week periods. Test solutions comprised 0.041 - 12 M HNO_3 and 0 - 3 M NaCl. The OCP for each sample was monitored for a one week period. Representative OCP data are shown in Figure 1. Three distinct types of behavior were observed for 304 SS. The first type of behavior included samples whose initial potentials were relatively noble (> -0.2 V_{SCE}) and became more positive with time until a steady state potential was attained (Figure 1, type 1). The second type was OCPs which were initially negative (< -0.3 V_{SCE}), gradually became more positive, and then displayed a rapid and large increase in potential (type 2). The third type of OCP behavior was similar to the second except that no sharp increase in potential was observed (type 3). No visible changes in the solutions were observed following type 1 behavior. In contrast, solution chemistries promoting types 2 and 3 behavior ranged from faint translucent yellow-green to opaque dark green. These solution appearances are consistent with salt solutions of the metal components comprising 304 SS, Fe, Ni, and Cr. Thus, the appearance of type 2 and 3 solutions suggests significant dissolution.

As an initial step in delineating corrosion behavior, weight loss measurements were performed. The results, combined with OCP measurements and observed solution color, allow a preliminary analysis of the surface state (active or passive) of 304 SS in different environments. It was observed that samples revealing type 1 OCP behavior had weight losses that were extremely low (< 1 mg on > 1 g samples). Conversely, samples revealing types 2 or 3 behavior had much larger losses. Weight loss data following one week exposure to each solution are displayed as average corrosion rates in Figure 2[1]. The consequences of presenting an average corrosion rate are discussed below.

The surface state of 304 SS during exposure to the various environments can be inferred from the OCP and weight loss data. The combination of data sets suggests samples that displayed type 1 behavior, i.e. those that maintained a noble OCP and had negligible weight loss, were continuously passive following immersion. Conversely, the OCP, solution appearance, and weight loss data suggest that active corrosion is occurring for types 2 and 3 behavior. The question arises as to the jump in potential for type 2 behavior. This behavior, previously observed by Mirolyubov *et al*., was theorized to result from a spontaneous active/passive transition.[25] They reasoned that such a transition was logical in light of the autocatalytic nature of HNO_3 reduction, discussed by Evans[26]. The autocatalytic reduction of HNO_3 arises from the geometric increase in the production of the oxidant NO_2 by means of one of two possible mechanisms, both of which have the same net reaction:[27]

$$HNO_3 + H^+ + e^- \rightarrow NO_2 + H_2O \quad (1)$$

One mechanism, termed the heterogeneous mechanism, has been shown to occur exclusively at more anodic potentials (> 0.5 V_{SCE} in boiling 8 M HNO_3):[27]

$$NO_2 + e^- \rightarrow NO_2^- \quad (2)$$

$$NO_2^- + H^+ \rightarrow HNO_2 \quad (3)$$

$$HNO_2 + HNO_3 \rightarrow 2NO_2 + H_2O \quad (4)$$

The second mechanism, the homogeneous mechanism, was shown to occur in parallel with the heterogeneous mechanism at lower potentials:[27]

$$HNO_2 + H^+ \rightarrow NO^+ + H_2O \quad (5)$$

[1] Where replicate experiments were performed, the corrosion rate represents an average of the tests.

$$NO^+ + e^- \rightarrow NO \quad (6)$$

$$NO + HNO_3 \rightarrow HNO_2 + NO_2 \quad (7)$$

For either mechanism, reduction of HNO_3 is autocatalytic, generating oxidant at a geometrically increasing rate.[2]

Based on the aforementioned observations, it is conceivable that the spontaneous passivation may be attributable to 1) cation dissolution, 2) cation oxidation by HNO_3 in solution, and 3) cation reduction at the working electrode surface. Dissolution would be autocatalytic because cations oxidized by solution would be available for reduction, thus increasing metal dissolution. (This assumes that cation oxidation by solution is not rate limiting.) However, this mechanism is unlikely in room temperature solutions because oxidation of the pertinent metal cations by nitrate is not observed in acidic solutions.[38,39,40] Autocatalytic corrosion via solution oxidation of metal cations is plausible at higher temperatures, and this mechanism may be explored in the future.

In order to confirm that the three types of OCP behavior were attributable to continuously passive, active/passive, and active surface states, potentiodynamic scans were performed (Figure 3). Three of the polarization curves displayed in Figure 3 were generated using solutions of different composition and were initiated following 4 hours at OC. The three different solutions, 0.4 M HNO_3 + 0.1 M NaCl, 1.2 M HNO_3 + 0.3 M NaCl, and 0.4 M HNO_3 + 1 M NaCl, promoted what was hypothesized to be continuously passive, active/passive, and active behavior, respectively. The fourth curve was generated using a solution identical to one of the other three (1.2 M HNO_3 + 0.3 M NaCl), but the scan was initiated following a 2 day immersion at OC. The polarization curves confirmed that solutions promoting OCP behavior consistent with continuous passivity (0.4 M HNO_3 + 0.1 M NaCl) indeed yielded passivity and solutions promoting OCP behavior consistent with continuous active corrosion (0.4 M HNO_3 + 1 M NaCl) resulted in active corrosion. To check the validity of the hypothesis that the rapid increase in OCP is attributable to an active/passive transition, two anodic polarization scans using 1.2 M HNO_3 + 0.3 M NaCl were performed. One scan was initiated before the rapid increase in OCP (4 hour immersion at OC) and the other after the increase (2 day immersion at OC). The 4 hour pretreatment scan reveals an actively corroding working electrode, while the 2 day scan shows a passively dissolving electrode, as evidenced by the low corrosion current density, generally potential independent current density

[2] Truman[37] showed that in the case of boiling 65% HNO_3, the presence of NO_2 actually inhibits corrosion by reducing the Cr^{6+} in solution (created via oxidation by HNO_3) to Cr^{3+}, thus preventing Cr^{6+} reduction at the working electrode. However, oxidation of Cr^{3+} to Cr^{6+} in room temperature HNO_3 solutions is negligible.[38]

which is less than 10^{-5} A/cm^2, and electrochemical impedance spectroscopy (not shown). Therefore, the polarization curves confirm that the rapid increase in OCP is attributable to spontaneous passivation, that relatively negative OCPs are attributable to active corrosion, and that noble OCPs are attributable to passive dissolution. The origin of the alternating net cathodic and anodic current measurements during anodic polarization is discussed in the "Active/Passive Transition" section below. Additionally, although some tests were active over the entire one week testing period, they were found to eventually passivate. Thus, it can be stated that continuously active behavior is identical to active/passive behavior, with the apparent differences arising from the chosen test period. It is probable that some solution combination never yields spontaneous passivity of 304 SS but such a solution was not discovered in this study.

Because the source of the rapid increase in OCP is attributable to the autocatalytic nature of HNO_3 reduction, increasing corrosion rates should be observed during periods when active corrosion is occurring. In order to validate this assertion, a 304 SS sample was immersed in 1.2 M HNO_3 + 0.3 M NaCl while the OCP was monitored. A linear polarization resistance measurement was generally performed every 4 hours. The results are shown in Figure 4. It was found that the polarization resistance decreased with time preceding the jump in the OCP (OCP < -0.2 V_{SCE}). The corrosion rate, which is inversely proportional to polarization resistance, increased exponentially with time. The corrosion rate increased by more than 2 orders of magnitude before passivation occurred (at approximately 25 h). This result supports the theory that corrosion at OC is autocatalytic. The logarithm of the polarization resistance varied linearly with potential preceding the OCP increase, indicative of Tafel-like, and thus active, behavior. Additionally, a marked decrease in corrosion rate (approximately 4 orders of magnitude) was observed following the OCP step. This is further evidence that the sharp increase in OCP is attributable to passivation. Further, electrochemical impedance spectra (not shown): 1) confirmed the polarization resistance measurements, 2) were consistent with active surface spectra (with an adsorbate) preceding the OCP jump, and 3) were consistent with passive film spectra following the OCP increase. In summary, these results are evidence of autocatalytic corrosion of 304 SS exposed to HNO_3/NaCl, which to date has been hypothesized but has never been directly shown.

Active/Passive Transition

Dependence of active/passive transition on V:A ratio

Additional tests were performed in order to examine the autocatalytic nature of HNO_3 reduction. Dissolution control by autocatalytic HNO_3 reduction implicitly assumes that passivation

arises from changes in solution chemistry rather than alteration of the SS surface structure or composition. This distinction is important, because evidence in the literature has shown that the improved corrosion resistance of SS following immersion in aqueous HNO_3 solutions is imparted by dissolution of inclusions[41] and/or chromium enrichment of the surface[42].

If spontaneous passivation is attributable to autocatalytic reduction of HNO_3, or more specifically reduction of NO_2 and NO (see Equations 1-7), then introduction of NO_2 or NO gas into solution should promote passivity. To test this hypothesis, a solution which promotes active dissolution upon immersion of a 304 SS (4.1 M HNO_3 + 1 M NaCl) was continuously sparged with NO_2, beginning 2 hours prior to immersion of a 304 SS sample. The OCP was monitored for 4 hours, followed by initiation of an anodic polarization scan. The OCP and polarization data (Figure 5) indicate that 304 SS is spontaneously passive upon immersion in NO_2 sparged 4.1 M HNO_3 + 1 M NaCl. Similar results were observed with NO sparged solutions (see Figure 5). Immediate passivation upon immersion in NO_2 and NO sparged solutions is consistent with the assertion that autocatalytic reduction of HNO_3 is responsible for spontaneous passivation of 304 SS. Immediate passivation also indicates that solution chemistry governs spontaneous passivation.

The V:A ratio of 304 SS exposed to 4.1 M HNO_3 + 1 M NaCl was varied to determine whether spontaneous passivation is dependent on reaction product concentration. It was expected that decreasing the V:A ratio would increase the reaction product concentration in solution and therefore decrease the time required for spontaneous passivation. As shown in Figure 6, this predicted result was observed, and is similar to that noted previously.[25] The observed concentration dependence is consistent with the notion that solution chemistry governs spontaneous passivation. Additionally, the time required for spontaneous passivation did not increase linearly with V:A ratio. The dependence of passivation time on volume was more consistent with an exponential dependence **(**t_{pass} proportional to $10^{(V:A)}$**)**, which would be expected in light of the autocatalytic reduction mechanism driving passivation.

A third test was utilized to examine the effect of solution chemistry on passivation. A 304 SS sample was immersed in aerated 4.1 M HNO_3 + 1 M NaCl for 24 hours, with passivation occurring after 5.6 hours. The sample was then removed from solution and immediately immersed in fresh, aerated 4.1 M HNO_3 + 1 M NaCl. OCP measurements following the immersion in fresh solution were similar to those observed upon the initial immersion; i.e., the OCP started out relatively negative and displayed a sharp increase around 5.6 hours. This result suggests that solution chemistry, as opposed to surface composition, governs spontaneous passivation of 304 SS in HNO_3 / NaCl environments.

If the solution chemistry is entirely responsible for spontaneous passivation of 304 SS then a second, fresh sample should passivate in the same solution. In order to test this, a sample was immersed in 125 ml of 4.1 M HNO_3 + 1 M NaCl for approximately 69000 s, with passivation occurring approximately 1400 s after immersion. The initial sample was removed and a second sample then immersed. This sample required 2500 s to passivate. It was believed that the lack of immediate passivation might be due to changes in solution chemistry, because 67600 s had elapsed before the second sample was immersed. This seemed logical in light of the fact that the oxidizing agents responsible for the autocatalytic behavior are unstable and are known to decompose with time.[26,43] Indeed, other researchers have noted an effect of sealing the test cell to prevent egress of reaction products.[2] Because passivation drastically reduces the corrosion rate, and thus the production of oxidizing species, it appeared likely that the steady state concentration of oxidizers would be diminished. Therefore, a third sample was immersed in solution immediately following passivation. This sample passivated immediately. (These results were confirmed by replicate testing.) An interesting conclusion from this series of tests is that, well after passivation has occurred, the oxidizer concentration is sufficient to maintain passivity but is insufficient to promote passivity of a freshly immersed sample. Thus, there appears to be an effect of surface state on spontaneous depassivation. However, the previous series of tests suggests that the solution chemistry is generally responsible for spontaneous passivation.

Effect of the active/passive transition on corrosion rate determination by weight loss tests

The question arises as to the meaning of the average corrosion rates for materials that display an active/passive transition (Figure 2). It was shown above that the instantaneous corrosion rate is dependent upon V:A ratio and time, with the corrosion rate increasing roughly exponentially until passivation (Figure 4). For tests exhibiting an active/passive transition, nearly all of the dissolution occurs during the period of active corrosion because the corrosion rate is many orders of magnitude smaller during passive corrosion. Thus, the corrosion rates reported in Figure 2 are only valid as average corrosion rates over a one week period in 400 ml solution. Therefore, the representation of an average corrosion rate is somewhat misleading without explicit knowledge of the conditions that yielded the result because the corrosion rate varies over many orders of magnitude. Extrapolation of the data to service conditions must be done quite carefully when operating in solutions that promote a spontaneous active/passive transition.

The corrosion rate obtained from weight loss tests can be misleading because weight loss is cumulative. Weight loss measurement yield an average corrosion rate over time, even though the

instantaneous corrosion rate varies over many orders of magnitude. Because of the variation in instantaneous corrosion rate, the length of the testing period will affect the average corrosion rate measured from weight loss. An example of the variability of corrosion rate measurements from weight loss testing is shown in Figure 7. The corrosion rate that would be obtained from weight loss measurements on 304 SS exposed to 4.1 M HNO_3 + 1 M NaCl can be calculated as a function of V:A ratio and test time, assuming that the potential increases linearly with time until passivation. Figure 7, which shows the results of this calculation, indicates that the average corrosion rate determined by weight loss tests can vary between 0.17 and 35,000 mpy depending upon test conditions. During active corrosion, the average corrosion rate increases with test period because the instantaneous dissolution rate increases exponentially with time. However, following spontaneous passivation, the average corrosion rate decreases with test period as a result of the dramatically lower dissolution rate during passive dissolution. The average corrosion rate would be maximized when the test period is equal to the time required for spontaneous passivation. Thus, variation in experimental procedure can result in dramatically different results when using weight loss measurements alone to determine the corrosion rate. It is this phenomenon that makes assembly of the weight loss data in the literature practically impossible due to the variety of conditions employed. Indeed, the need for a single unified study was one impetus for this work. In summary, observed corrosion rates following immersion may be misleading and weight loss measurements cannot be readily extrapolated to service conditions.

Origin of active/passive transition

It is conceivable that the spontaneous passivation is due to salt film precipitation and not to spontaneous oxide film formation. However, there are a variety of arguments against salt film formation causing spontaneous passivation. First, assuming a linear diffusion gradient from the surface, the surface concentrations of dissolved SS ($1.5x10^{-4}$ to 0.3 M) salts are, at a minimum, an order of magnitude too low to yield precipitation at the surface.[44,45,46,47] Moreover, when the dissolution current density is relatively large, salt film precipitation would be attributable to exceeding the salt solubility in the near surface region only, with the bulk solution concentration below that required for salt film precipitation. If this salt film precipitation occurred, subsequent salt film dissolution would be expected as a result of the dramatic decrease in anodic current density which would reduce the near surface salt concentration to a level roughly equivalent to that of the subsaturated bulk solution[47,48,49] (cation concentrations of 10^{-4} to 0.1 M). However, oscillation of current density (on the order of mA/cm^2), which is observed for periodic salt film precipitation/dissolution cycles[47,48,49], is not observed here. Further, the passivation events do not correlate with particular near surface salt concentrations. Rather the concentrations vary by many

orders of magnitude. Therefore, the rapid decrease in corrosion rate does not appear to arise from salt film formation but rather from passive film formation.

Effect of the active/passive transition on anodic polarization behavior

The origin of the alternating net cathodic and anodic behaviors observed during anodic polarization (see, for example, Figure 3) is explained by the fact that anodic polarization triggers passivation. The passivated surface has an OCP far more noble than the OCP upon initial immersion (see Figure 3). This behavior arises from the fact that the cathodic branch crosses the anodic branch in three places: in the active corrosion region, on the electrically unstable side of the passivation nose (the region where current decreases with increasing potential), and in the passive region. Thus, following passivation of the surface, potentials that were previously anodic to the original (primary) OCP become cathodic to the new (secondary) OCP. This is evident from Figure 8, which shows two separate anodic and cathodic polarization curves, both acquired following 4 hours at OC. The anodic and cathodic data which cannot be observed due to the predominance of the corresponding opposite reaction (dashed lines in Figure 8) are inferred and sketched for clarity. (The two different cathodic slopes observed result from a change in reaction mechanism, as discussed by Razygraev *et al.*[27]) The mixed potentials resulting from the intersections of these lines indeed yield the observed OCPs. Thus, the source of the alternating anodic and cathodic behavior arises from multiple intersections of the anodic and cathodic curves.

The exact reactions that result in the secondary OCP (i.e., that observed following passivation) observed on samples displaying an active/passive transition have not been rigorously examined in this study. It appears likely that the secondary OCP results from a mixed potential of anodic passive dissolution and cathodic NO_3^- and/or NO_2 reduction. This hypothesis arises from the fact that the anodic reaction appears to be passive dissolution, practically identical to that observed on spontaneously passive samples (Figure 9). The cathodic reaction is likely reduction of nitrogen species (Equations 1-7) because proton or water reduction is thermodynamically precluded at these relatively noble potentials and the current densities are too large for oxygen reduction, which is mass-transport limited. It is possible that the OCP arises from a redox couple of nitrogen products on the SS surface, similar to what would be observed on an inert electrode exposed to HNO_3. However, this would require that: 1) the anodic reaction is mass-transport limited, 2) the mass-transport limited current density is identical to the passive current densities observed on spontaneously passive materials, and 3) the redox couple is independent of solution composition, which seems highly unlikely. A redox couple arising from dissolved SS cations is also unlikely for the same three reasons given above. Additionally, although the Fe^{2+}/Fe^{3+} redox

couple has been observed on 304 SS[50] in a solution containing 0.35 M Fe ions, the Fe concentrations following passivation during potentiodynamic polarization are as low as 1.8×10^{-5} M (based on q_{anodic} preceding passivation, Table 1). This would yield an exchange current density of 10^{-11} A/cm^2.[50] The current observed at the secondary OCP is much larger. Thus, it appears that the secondary OCP arises from the mixed potential comprising anodic dissolution and cathodic reduction of nitrogen compounds. However, further studies are required to confirm this hypothesis.

Effect of the time required for spontaneous passivation on the pit initiation time

Because pitting requires an otherwise passive surface by definition, it may be stated that no pitting may occur during active dissolution. Thus, the critical time required for pitting must be tempered by an additional temporal factor, i.e., the time required for passive film formation. This time component should not be confused with the classical definition of pit initiation time (which arises from the time required to develop a localized chemistry that can locally depassivate the surface), especially because the time required for passivation has been shown to be V:A ratio dependent. Thus, in the case of 304 SS exposed to HNO_3 / NaCl environments, the pit initiation time ($\tau_{pit\ initiation}$) is comprised of two components:

$$\tau_{pitinitiation} = \tau_{passivation} + \tau_{localizedchemistry} \qquad 8$$

Evidence for this phenomenon is demonstrated in Figure 10. Micrographs were taken following immersion of three separate samples in 4.1 M HNO_3 + 1 M NaCl. One sample was immersed for 5.6 hours and removed preceding passivation, as determined by its OCP. The second sample was immersed for 24 hours, the final 17.5 hours of which the sample was passive, as determined by OCP measurement. The third sample was immersed for 168 hours total, the final 163 hours of which the sample was passive. The micrographs show that no pitting was observed on the sample removed while actively corroding (Figure 10a) or the sample removed following 17.5 hours in the passive state (Figure 10b). Conversely, pits were observed on the sample exposed for 168 hours (Figure 10c)[3]. Therefore, two different components of the induction time for pitting are observed, one for spontaneous passivation and another for localized chemistry development.

[3] The pits appear to be crystallographic in nature, displaying four-fold symmetry. The pits appeared to occur only on sharply faceted grains. Preliminary evidence suggests that these grain faces were {111} planes. Replicate tests indicated that crystallographic pitting is reproducible.

HNO_3 and NaCl Concentration Effects on the Corrosion Behavior of 304 SS

The OCPs measured at the end of each one week test period are plotted in Figure 11. Statistical analysis (linear regression from 32 observations) of the data suggests that the dependence of OCP is most consistent with the following equation:[4]

$$OCP\ (V_{SCE}) \quad = \quad 0.39 + 0.31 * \log[\ HNO_3\ ] - 0.04 * \log[NaCl] \qquad 9$$

where [HNO_3] and [NaCl] are concentrations given in M. The analysis suggests that increasing the HNO_3 concentration increases the OCP (confidence > 99.9999%). This result is not surprising because the nitrate anion is a strong oxidizer. Conversely, the analysis suggests that OCP becomes more negative with increasing NaCl concentration, but this cannot be stated with high confidence (i.e., confidence is < 95%). However, other authors have noted a more negative OCP with increasing NaCl.[22,51]

The average corrosion rates observed from one week immersions of 304 SS in various aerated solutions are shown in Figure 2. As discussed above, the average corrosion rate can be misleading because the corrosion rate during active corrosion is increasing exponentially with time and because the corrosion rate incorporates periods of active and passive dissolution. However, when examined in conjunction with other data such as maximum corrosion rates, Flade potentials (potential at which the current no longer decreases with increasing potential), and average active corrosion rates, average corrosion rates can be instructive in a qualitative sense.

Figure 12 shows the average corrosion rates during the active corrosion period. These values were obtained by dividing the thickness loss (determined by weight loss measurement) by the time of active corrosion (determined by OCP measurement, Table 2). Thus, the calculations attribute the total weight loss to active corrosion, which leads to only a very small error for one week immersions (see Figure 4). Both Figure 2 and Figure 12 show that increased NaCl concentrations promote a larger active corrosion rate. This result is supported by potentiodynamic scans (Figure 13) which indicate that increasing the NaCl concentration increases the peak (nose) current density and Flade potential, while lowering the OCP. Thus, the maximum current density, the overpotential required for passivation, and the total anodic charge loss (Table 3) during active corrosion increase with NaCl concentration. The corrosion current density following 4 hours at OC also increases with NaCl concentration. In contrast, the passive current density varies little

[4] The analysis did not include OCP measurements at one week for the two solution chemistries that did not promote passivity within one week (0.04 M HNO_3 + 3 M NaCl and 0.41 M HNO_3 + 1 M NaCl). Because the one week test period was arbitrary and because these solutions eventually yielded passivity, the values were not included.

with NaCl concentration for tests wherein passivity is observed upon initial immersion (Figure 14). The tests in Figure 14 show that the OCP becomes more negative with increasing NaCl at four hours, similar to the results seen after one week immersions (Figure 11). As would be expected, increasing NaCl concentration increases the susceptibility to pitting (for example, compare 0.041 M HNO_3 + 0.3 M NaCl (Figure 9, no pitting) and 0.041 M HNO_3 + 1 M NaCl (Figure 15, pitting)). This has been observed by others.[30]

Similarly, the effect of HNO_3 concentration on the corrosion behavior of 304 SS can be discerned. Figure 2, Figure 12, and Table 3 indicate that increasing HNO_3, up to 4.1 M, increases the total anodic charge passed prior to passivation, as well as the average corrosion rate while active. This is consistent with polarization data (Figure 9, Figure 15) which reveal that increased HNO_3 concentrations promote a higher peak current density and more noble Flade potential. Thus, both NaCl and HNO_3 have the same effect on active corrosion, increasing the corrosion current density, increasing the maximum current density prior to passivation **(**$\log(i_{max}) = -2.1 + 2.3*\log[HNO_3] + 1.9*\log[NaCl]$, >96% confidence, 0.12 M - 4.1 M HNO_3 and 0.3 M - 1 M NaCl**)**, and decreasing the passive potential range. Unlike NaCl concentrations, though, HNO_3 concentrations generate maximum dissolution at intermediate levels. An increase in HNO_3 concentration from 4.1 M to 12 M (or a transition from active to passive within a single solution such as 4.1 M HNO_3 + 1 M NaCl) can reduce the corrosion rate by as much as 5 orders of magnitude. The transition from active to passive corrosion between 4.1 M and 12 M HNO_3 is consistent with weight loss measurements by Ondrejcin and McLaughlin[16], who showed that the boundary between passive and active dissolution upon immersion varied between 6 M and 11 M HNO_3 for HF concentrations of 0.1 M - 2 M[16]. Others have also noted spontaneous passivation upon immersion when the HNO_3 concentration exceeded 3 M.[21,52] A complex dependence of passivation on HNO_3 concentration is not surprising in light of the opposite effects of increasing acidity[1] and increasing NO_3^- [23]. However, in contrast to active corrosion, the passive current density is seen to vary little with HNO_3 concentration. Additionally, increasing HNO_3 increases the OCP following 4 hours in solution (Figure 9, Figure 15), similar to that observed during one week immersion tests.

Increasing HNO_3 beyond 0.0041 M eliminated pitting in 0.3 M NaCl solutions (Figure 9). The repassivation potential was more negative in the presence of 0.0041 M HNO_3 (0.041 V_{SCE}) than in the absence of HNO_3 (0.085 V_{SCE}). See Table 4. Therefore, as with general corrosion, maximum susceptibility to pitting occurs at intermediate HNO_3 concentrations. That is, the pitting potential decreases with increasing HNO_3 concentration until the concentration exceeds some

critical concentration beyond which pitting is not observed at all.[5] Note that although the scan reversal current densities varied (either 10^{-2} or 10^{-3} A/cm^2), comparison of separate tests incorporating the two different reversal current densities indicated no discernible variation in E_{rp}. The lack of dependence of E_{rp} on reversal current density was noted regardless of solution chemistry.

The active/passive boundary (the demarcation between solutions that generate spontaneous passivity of 304 SS upon immersion and those that yield activity) is complex, with active corrosion susceptibility at intermediate HNO_3 concentrations (see Figure 2). In contrast to the boundary for the critical concentration of Cl^- for pitting (as a function of $NaNO_3$ concentration)[30], the active/passive boundary cannot be defined by a simple first order equation. The lack of a defining simple first-order equation is not surprising because the critical Cl^- concentration required for pitting is thought to arise from competitive adsorption with NO_3^- anions[28,30,32], while the active/passive boundary is determined by mixed potential theory which by nature is complex when the anodic branch exhibits active/passive behavior and the cathodic kinetics are continuously changing.

Research by Mirolyubov *et al.*[25] indicated that the time required for spontaneous passivation increased with increasing Cl^- and decreasing HNO_3. Regression analysis of spontaneous passivation times in this study (18 separate observations, including replicate tests) confirmed that increasing chloride concentration inhibited spontaneous passivation. However, results from our study indicate that the time required for spontaneous passivation (Table 2) is greatest at intermediate concentrations of HNO_3. Such a result is logical in light of the fact that active corrosion is only observed at intermediate HNO_3 concentrations. The results from the present study do not obviate those of Mirolyubov *et al.* because those researchers investigated only a small range of HNO_3 concentration (1 M - 5 M). This study appears to corroborate decreasing passivation time with increasing HNO_3 concentration over this range.

It is interesting to note that no single critical anodic charge density (Table 1 and Table 3), current density (Figure 9 and Figure 15), potential (Figure 9 and Figure 15), or time (Table 2) is required for spontaneous passivation. All of these critical values vary with HNO_3 and NaCl. This is not surprising since passivation is a function of NO_3^- concentration[23] and pH[1], which have

[5] This result does not obviate the results of Leckie and Uhlig[30] who showed that the critical Cl^- concentration for pitting increases with increasing $NaNO_3$ concentration, since that research did not examine pitting potential or repassivation potential.[30] That is, their research determined the boundary between pitting and nonpitting, but did not examine the effect of NO_3^- and Cl^- on the repassivation potential within the pitting regime. Comparison of the data from this study to that of Leckie and Uhlig ($NaNO_3$/NaCl) is difficult, given the dramatic differences in pH.

opposite effects, as well as Cl^- concentration[2]. In light of the proposed mechanism of passivation, it may be concluded that for a particular NO_3^- concentration, Cl^- concentration, and pH, a critical oxidant concentration is required for passivation. The precise oxidant concentration and its dependence upon pH, NO_3^-, and Cl^- are unknown at this time.

Temperature Effects on the Corrosion Behavior of 304 SS

The effects of temperature on the corrosion behavior of 304 SS exposed to HNO_3 / NaCl environments were examined using potentiodynamic polarization. Representative elevated temperature tests are shown in Figure 16 and Figure 17. Increasing the temperature from room temperature (22°C) to boiling (94°C and 101°C (sea level)) increased the tendency toward activation of the surface following 4 hours at OC. Increasing temperature increased both the anodic and cathodic kinetics, as would be expected. However, during active corrosion, the increase in anodic kinetics is greater than the increase in cathodic kinetics, as evidenced by the increased corrosion current density and decreased OCP. The maximum anodic current density was also seen to increase with temperature. Thus, the effect of increasing temperatures is to increase the active/passive nose current density and to decrease the OCP, thereby exposing the active branch of the anodic polarization curve. Analogous to room-temperature tests, increasing HNO_3 concentration increased both the active/passive nose current density and the Flade potential (compare Figure 16 and Figure 17). Moreover, temperature increases resulted in larger passive current densities (see Figure 16).

Increasing temperature also promoted pitting susceptibility, as seen in Figure 16. The pit initiation and repassivation potentials were found to decrease with temperature following statistical analysis of replicate tests. (Pitting and repassivation potentials are displayed in Table 4.) Also, following passivation, tests at 65°C and 94°C indicated that 304 SS pits at its secondary OCP. However, that was not the case for exposures at 55°C, where some anodic polarization was required to initiate pitting.

The types of corrosion behavior observed following exposure to a variety of solution combinations and temperatures are shown in Figure 18. Similar to room temperature experiments, some solutions promote active/passive behavior (Figure 18), even though the polarization curves following 4 hours at OC suggest passivity (Figure 17). This apparent discrepancy arises from the fact that spontaneous passivation occurs prior to the initiation of applied polarization at 4 hours. Increasing HNO_3 and NaCl concentrations promote active corrosion in the <1 M HNO_3 region. However, increasing the HNO_3 concentration beyond a certain concentration promotes

spontaneous passivity (e.g., 12 M HNO_3 + 0.1 M NaCl). This phenomenon is similar to that observed in room temperature environments where the maximum susceptibility to corrosion occurs at intermediate HNO_3 levels.

Conclusions

In an effort to delineate the chloride tolerance limits of HNO_3 process streams, the corrosion behavior of 304 SS exposed to HNO_3 / NaCl solutions was examined. It was found that some solution chemistries promoted active corrosion upon immersion. Corrosion in these solutions was observed to be autocatalytic, with the corrosion rate increasing exponentially with time and potential. Current densities as large as 0.2 A/cm^2 were found to be possible. Invariably, the period of active corrosion terminated following spontaneous passivation, resulting in a corrosion rate decrease as large as 5 orders of magnitude. Corrosion behavior was strongly dependent on the solution volume to surface area ratio. This phenomenon, coupled with other results, suggested that spontaneous passivation arises solely from solution chemistry, as opposed to changes in surface composition. However, the same cannot be stated for spontaneous depassivation.

Increasing NaCl was deleterious to the corrosion resistance of 304 SS at all temperatures examined, from room temperature to boiling. Increasing NaCl concentrations promoted active dissolution upon initial immersion, a larger anodic overpotential required for passivation, pitting, longer active corrosion periods, larger anodic charge densities preceding passivation, and larger corrosion current and peak current densities. In contrast, intermediate HNO_3 concentrations promoted active dissolution over all temperatures examined, with continuous passivity noted at HNO_3 concentration extremes. During active corrosion, increasing HNO_3 concentration increased anodic charge density, corrosion current density, and peak current density. The time required for spontaneous passivation was a maximum at intermediate HNO_3 concentrations. Susceptibility to pitting was the highest at intermediate HNO_3 concentrations; the pit initiation and repassivation potentials decreased with increasing HNO_3 until pitting susceptibility was entirely eliminated. Passive current densities were not affected by NaCl or HNO_3 concentration.

Increasing solution temperatures increased the susceptibility to both pitting and active dissolution. Higher temperatures resulted in increased corrosion current densities and peak current densities as well as lower pit initiation and repassivation potentials. Increasing temperature increased anodic kinetics more rapidly than cathodic kinetics.

HNO_3 / NaCl combinations that promote continuous passivity can be used safely with 304 SS. Other solutions promoting active/passive behavior may be considered safe under particular conditions, however the corrosion behavior is complex. Under these conditions, extrapolation of data from this study to service conditions must be performed with great care.

References

1) R.M. Davison, T. DeBold, and M.J. Johnson in "ASM Handbook, Vol. 13, Corrosion", ASM International, Metals Park, OH, p. 547 (1992).
2) L.L. Shrier, R.A. Jarman and G.T. Burstein, "Corrosion, 3rd edition", Butterworth Heinemann, London, p. 3:34 (1993).
3) M.G. Fontana, "Corrosion Engineering, 3rd edition", McGraw-Hill, New York, p. 226 (1986).
4) T. Yamamoto, S. Tsukui, S. Okamoto, T. Nagai, M. Takeuchi, S. Takeda, and Y. Tanaka, *Journal Of Nuclear Materials*, **228**, 162 (1996).
5) L.Y. Gurvich and A.D. Zhirnov, *Protection Of Metals*, **31,** 418 (1995).
6) W.H. Smith and G.M. Purdy, *Waste Management*, **15**, 477 (1995).
7) A.N. Kuzyukov, *Materials Science*, **30**, 42 (1994).
8) V. Kain, S.S. Shinde, and H.S. Gadiyar, *Journal Of Materials Engineering And Performance*, **3**, 699 (1994).
9) J.Y. Jeng, B.E. Quayle, P.J. Modern, W.M. Steen,and B.D. Bastow, *Corrosion Science*, **35**, 1289 (1993).
10) G.N. Salaita and P.H. Tate, *Corrosion*, **52,** 493 (1996).
11) H. Yashiro, K. Tanno, S. Koshiyama, K. Akashi, *Corrosion*, **52**, 109 (1996).
12) H. Grafen and D. Kuron, *Werkstoffe Und Korrosion*, **47**, 16 (1996).
13) H.S. Khatak , J.B. Gnanamoorthy, P. Rodriguez, *Met. Trans. A*, **27**, 1313 (1996).
14) S. Angappan, S. Sathiyanarayanan, G. Rajagopal, and K. Balakrishnan, *Bulletin Of Electrochemistry*, **12**, 48 (1996).
15) D.D. Macdonald, E. Sikora, M.W. Balmas, and R.C. Alkire, *Corrosion Science*, **38**, 97 (1996).
16) R.S. Ondrejcin and B.D. McLaughlin, Savannah River Laboratory Report # DP-1550, E.I. duPont de Nemours & Co., Aiken, SC, (1980).
17) P.M. Kranzlein, Savannah River Laboratory Report # DP-486, E.I. duPont de Nemours & Co., Aiken, SC (1960).
18) V.K. Zhuravlev, M.M. Kurpetov, and V.I. Oreshkin, *Protection of Metals*, **8**, 161 (1972).
19) P. Ciriscioli, J.M. York, and G.J. Dooley in "Industrial Applications of Titanium and Zirconium, ASTM STP 728", A.W. Kleefisch ed., ASTM, Philadelphia, PA, p. 138 (1981).
20) S.B. Schreiber and S.L. Dunn, Los Alamos National Laboratory Report # LA-11566-MS, Los Alamos, NM (1989).
21) E.L. Christensen and W.J. Maraman, Los Alamos National Laboratory Report # LA-3542, Los Alamos, NM (1969).
22) A.I. Matantsev, *Zhurnal Prikladnoi Khimii*, **33**, 1285 (1960).
23) A.P. Gorodnichii and R.G. Rozenblyum, *Protection of Metals*, **23**, 722 (1987).
24) M.C. Petit, D. Desjardins, M. Puiggali, A. El Kheloui and C. Clement, *Corrosion Science*, **32**, 1315 (1991).
25) E.N. Mirolyubov, A.P. Kazakov and M.M. Kurtepov in "Corrosion of Metals and Alloys", N.D. Tomashov and E.N. Mirolyubov eds., Israel Program for Scientific Translation, Jerusalem, p. 102 (1966).

26) U.R. Evans, *Trans. Farady Soc.*, **40**, 120 (1944).
27) V.P. Razygraev, R.S. Balovneva, E.Y. Ponomareva, and M.V. Lebedeva, *Protection of Metals*, **26**, 43 (1990).
28) N.D. Tomashov, G.P. Chernova, and M.Y. Rutten, *Protection of Metals*, **18**, 671 (1982).
29) T.F. Degnan in "ASM Handbook, Vol. 13, Corrosion", ASM International, Metals Park, OH, p. 1134 (1992).
30) H.P. Leckie and H.H. Uhlig, *J. Electrochem. Soc.*, **113**, 1262 (1966).
31) H.H. Uhlig and J.R. Gilman, *Corrosion*, **20**, 289t (1964).
32) S. Matsuda and H.H. Uhlig, *J. Electrochem. Soc.*, **111**, 156 (1964).
33) N.D. Greene and M.G. Fontana, *Corrosion*, **15**, 32t (1959).
34) W. Schwenk, *Corrosion*, **20**, 129t (1964).
35) J.D. Redmond in "Metals Handbook, Desk Edition", H.E. Boyer and T.L. Gall, eds., ASM International, Metals Park, OH, p. 15·2 (1985).
36) "Annual Book of ASTM Standards", Designation G3-89, Vol. 3.01, ASTM, Philadelphia, PA, p. 56 (1989).
37) J.E. Truman, *J. Appl. Chem.*, **4**, 273 (1954).
38) W.H. Smith and G.M. Purdy, *Waste Management*, **15**, 477 (1995).
39) G. Vanweert and Y.X. Shang, *Hydrometallurgy*, **33**, 255 (1993).
40) D. Nicholls, "Pergamon Texts in Inorganic Chemistry, Vol. 24: The Chemistry of Iron, Cobalt and Nickel", Pergamon Press, Oxford, p. 979 (1973).
41) M.A. Barbosa, A. Garrido, A. Campilho, and I. Sutherland, *Corrosion Science*, **32**, 179 (1991).
42) G. Hultquist, M., Seo, T. Leitner, C. Leygraf and N. Sato, *Corrosion Science*, **27**, 937 (1987).
43) "Handbook of Chemistry and Physics", D.R. Lide, ed., 71st edition, Chemical Rubber Publishing Co., Boca Raton, FL, p. 4-84 (1990-1).
44) Z. Szklarska-Smialowska, "Pitting Corrosion of Metals", NACE, Houston, TX, p. 360 (1986).
45) N.J. Laycock, M.H. Moayed and R.C. Newman in "Critical Factors in Localized Corrosion II", P.M. Natishen, R.G. Kelly, G.S. Frankel, and R.C. Newman, eds., The Electrochemical Society, Pennington, NJ, p. 68 (1996).
46) D. Dunn and N. Sridhar in "Critical Factors in Localized Corrosion II", P.M. Natishan, R.G. Kelly, G.S. Frankel, and R.C. Newman, eds., The Electrochemical Society, Pennington, NJ, p. 68 (1996).
47) T.R. Beck, *J. Electrochem. Soc.*, **129**, 2412 (1982).
48) J.L. Hudson, J. Tabora, K. Hrischer, and I.G. Kevrekidis, *Phys. Let. A*, **179**, 355 (1993).
49) S.G. Corcoran and K. Sieradzki, *J. Electrochem. Soc.*, **139**, 1568 (1992).
50) M. Stern, *J. Electrochem. Soc.*, **104**, 559 (1957).
51) I.L. Rozenfel'd and V.A. Kachanov, *Zaschita Metallov*, **4**, 367 (1968).
52) D.M. Kramarenko, E.V. Yegorikhin, M.N. Fokin, and B.M. Gusev in "10th International Congress on Metallic Corrosion, Vol. 5", Trans. Tech. Publications, Aedermannsdorf, Switzerland, p. 199 (1989).

NaCl \ HNO_3	0.12	0.41	1.2	4.1
1	0.12	1.1	37	780
0.3			0.56	1.9
0.1				0.14

Table 1 - q_{anodic} (C/cm^2) preceding passivation of 304 SS in aerated, 22°C HNO_3/NaCl environments calculated from potentiodynamic scans.

NaCl \ HNO_3	0.12	0.41	1.2	4.1
1	$3.7x10^5$	$1.5x10^6$	$2.4x10^5$	$2.1x10^4$
0.3	$1.1x10^4$	$3.8x10^4$	$7.4x10^4$	$1.4x10^4$
0.1			$1.2x10^4$	$2.5x10^4$
0.03				$9.5x10^3$

Table 2 - Time (s) required for spontaneous passivation of 304 SS in aerated, 22°C HNO_3/NaCl environments determined by OCP measurements. Values represent averages of replicate tests when pertinent.

NaCl \ HNO_3	0.12	0.41	1.2	4.1
1	26	400	510	690
0.3	7.4	7.3	91	170
0.1			13	140
0.03				0.48

Table 3 - q_{anodic} (C/cm^2) preceding passivation of 304 SS in aerated, 22°C HNO_3/NaCl environments calculated from weight loss measurements. Values represent averages of replicate tests when pertinent.

HNO_3 Concentration (M)	NaCl Concentration (M)	Temperature (^oC)	E_{pit} (V_{SCE})	E_{rp} (V_{SCE})
0	0.3	22	0.220±0.003	0.085±0.006
0.0041	0.3	22	0.179±0.011	0.041±0.009
0.041	0.3	55	0.085±0.003	-0.044±0.003
0.041	0.3	65	0.062±0.003	-0.070±0.003
0.041	0.3	94	0.020	

Table 4 - Pitting and repassivation potentials (V_{SCE}) as function of solution chemistry and temperature.

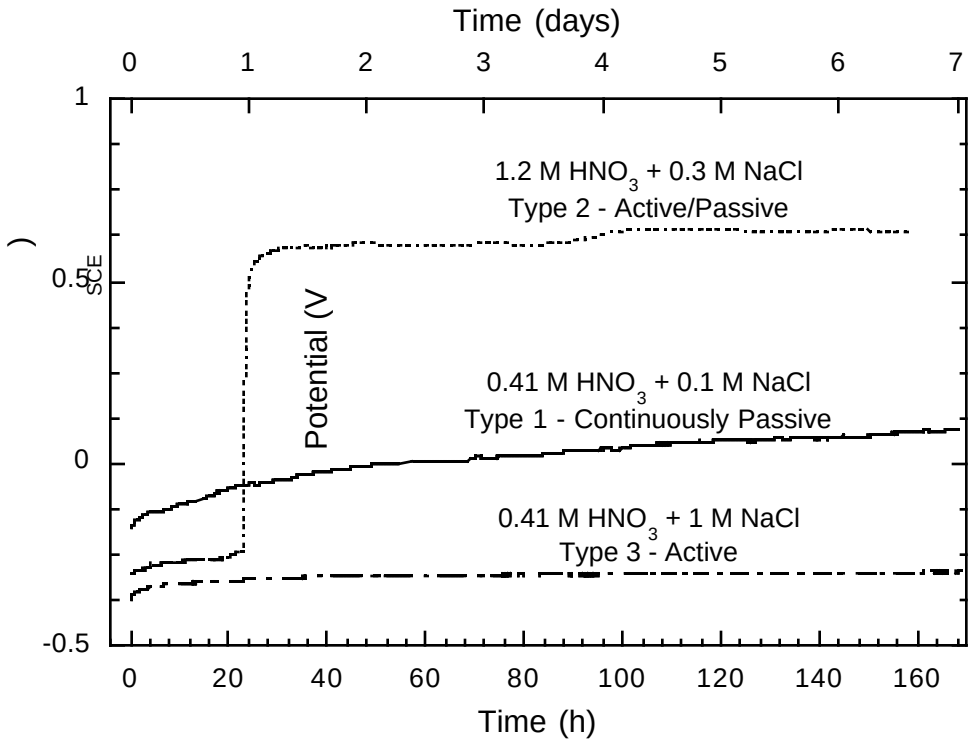

Figure 1 - Representative OCP data for different behavior types during one week immersions of 304 SS in aerated, 22° C, HNO_3 / NaCl environments. Each datum in this plot was recorded at 100 s intervals and represents an average of 1000 potentials measurements.

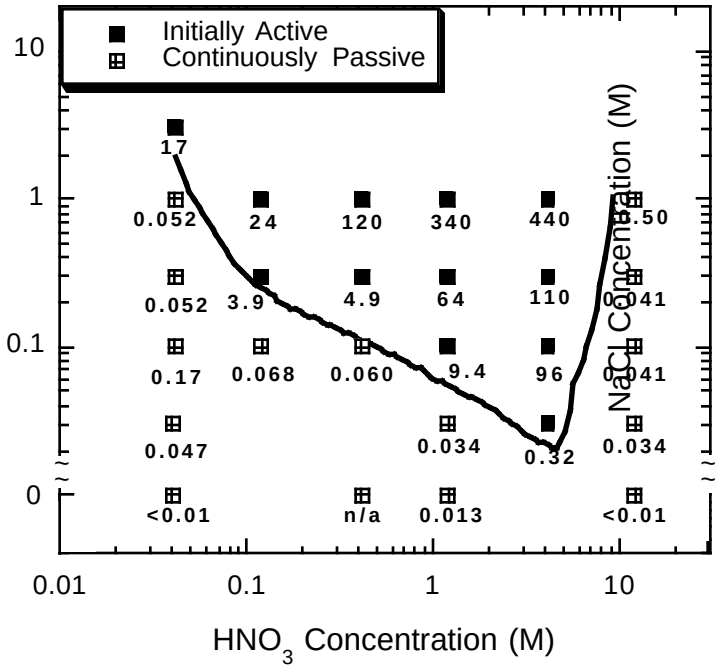

Figure 2 - Plot of surface states (active or passive) and average corrosion rates determined from one week tests incorporating 304 SS and aerated, 22°C, HNO_3/NaCl environments. Numeric values are the corrosion rates in mils per year.

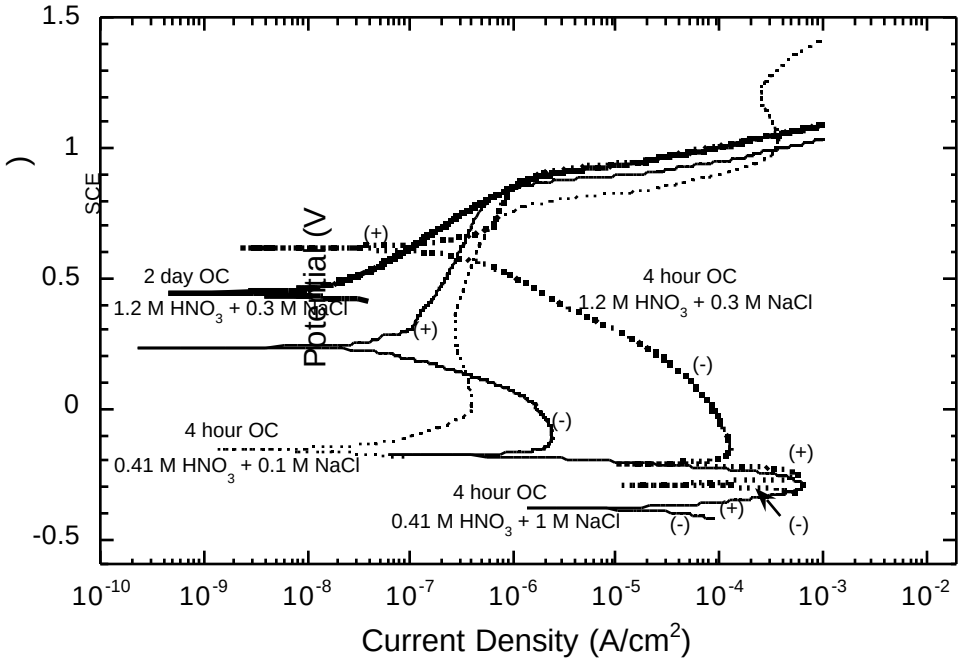

Figure 3 - Potentiodynamic scans on 304 SS exposed to different aerated HNO_3/NaCl solutions promoting the three observed types of behavior - passive, active/passive, and active. Minus (-) refers to portions of the scan in which the applied current is net cathodic. Plus (+) refers to portions of the scan in which the applied current is net anodic.

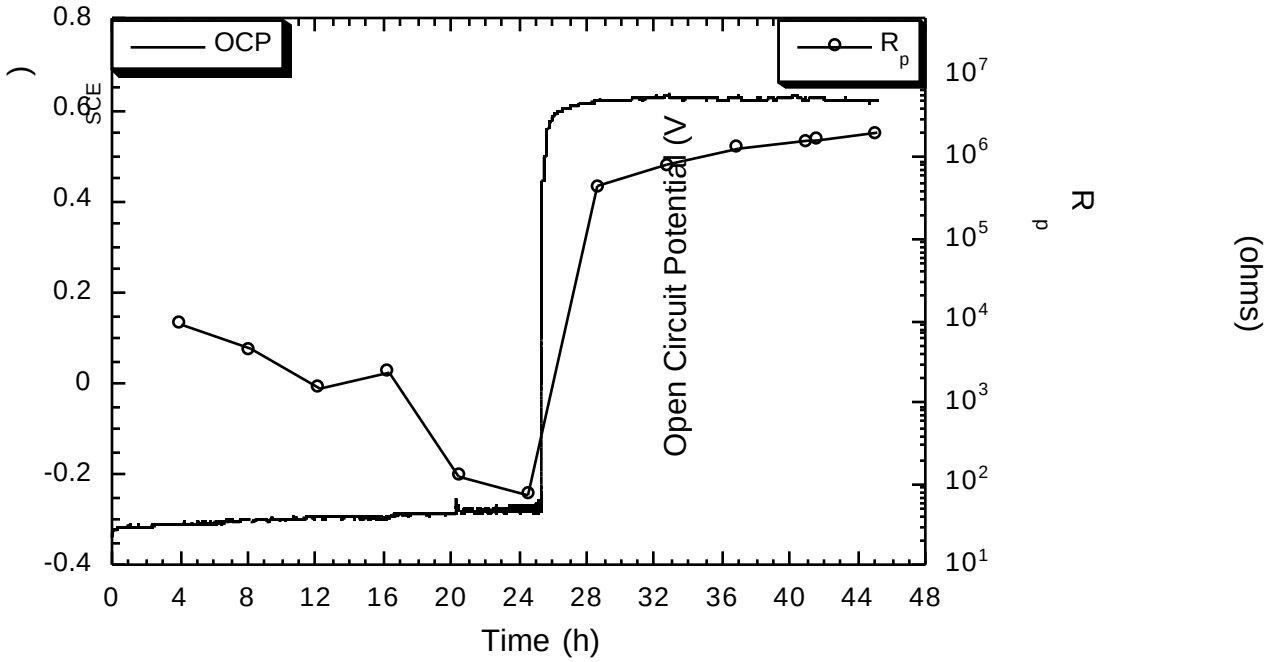

Figure 4 - Plot of OCP and polarization resistance (not corrected for area) as a function of time for 304 SS exposed to aerated, 22°C, 1.2 M HNO_3 + 0.3 M NaCl.

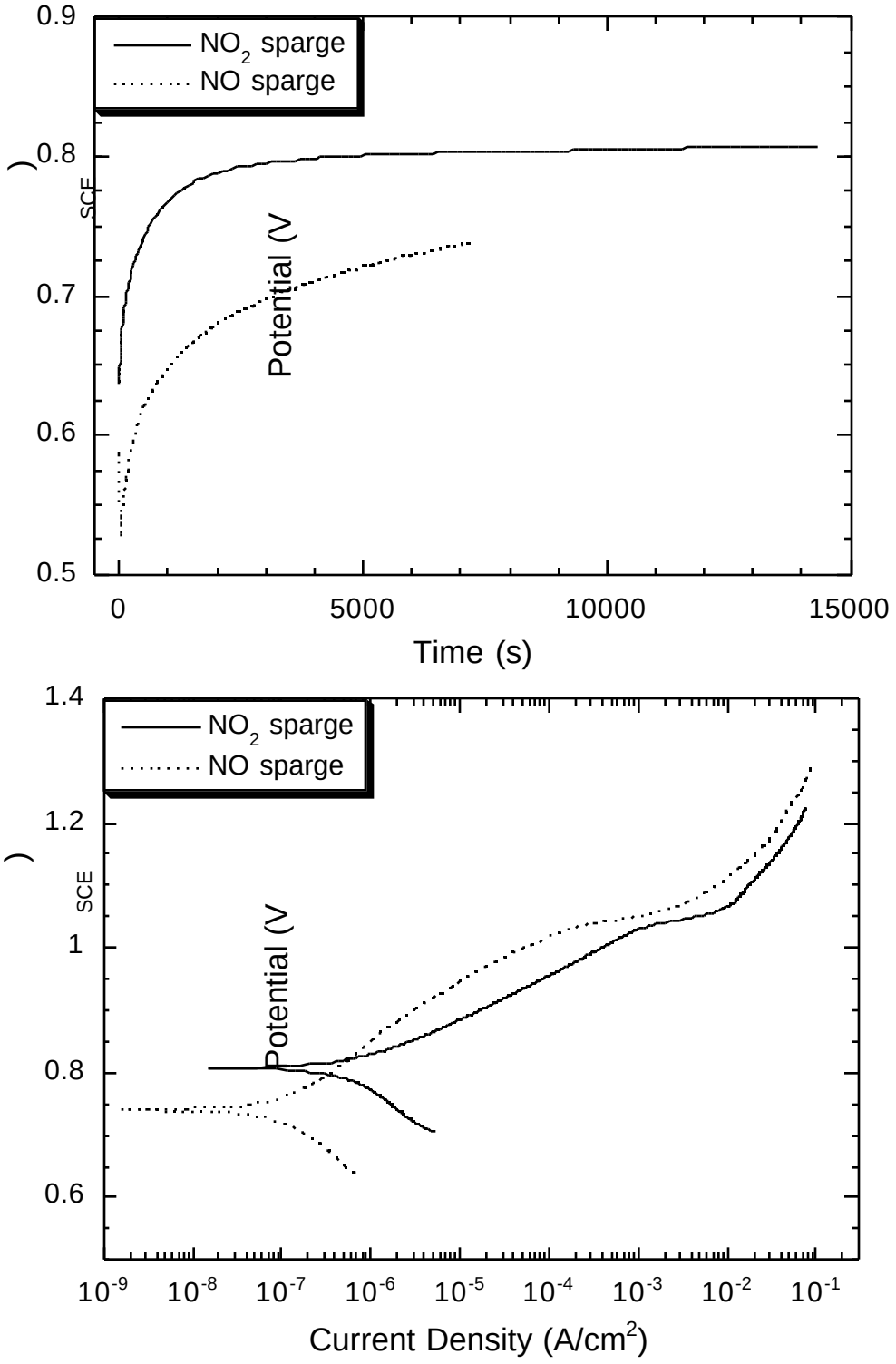

Figure 5 - a) OCP measurements upon immersion of a 304 SS electrode in 4.1 M HNO_3 + 1 M NaCl solutions sparged with NO_2 and NO. b) Anodic polarization measurements of 304 SS exposed to 4.1 M HNO_3 + 1 M NaCl solutions sparged with NO_2 and NO. The polarization measurements were initiated at the end of the OCP measurements shown in a).

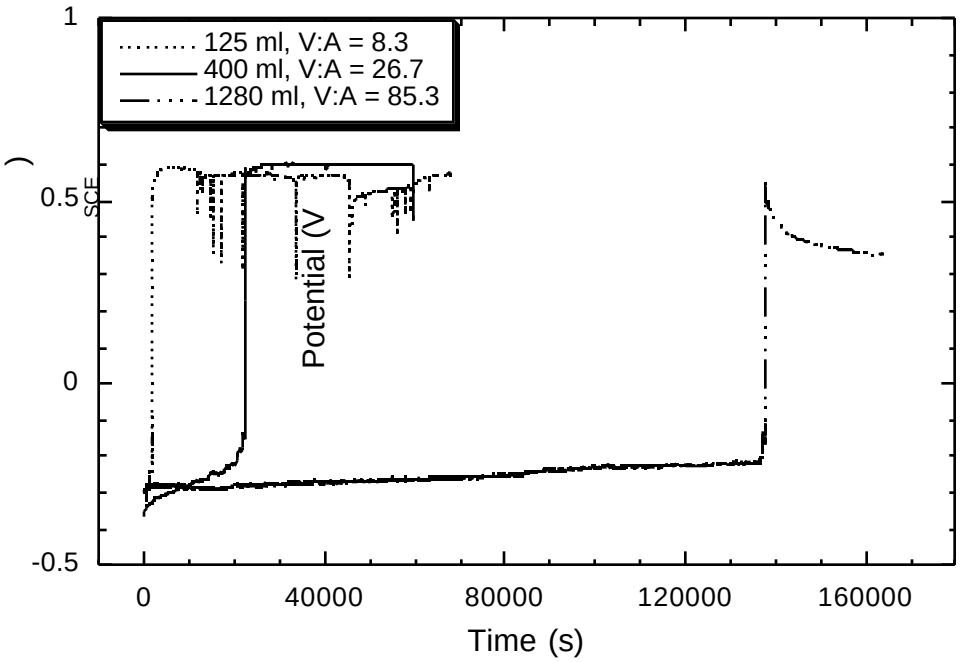

Figure 6 - OCP measurements of three 304 SS specimens (surface area = 15 cm^2) exposed to varying solution volumes of aerated, 22°C, 4.1 M HNO_3 + 1 M NaCl solution.

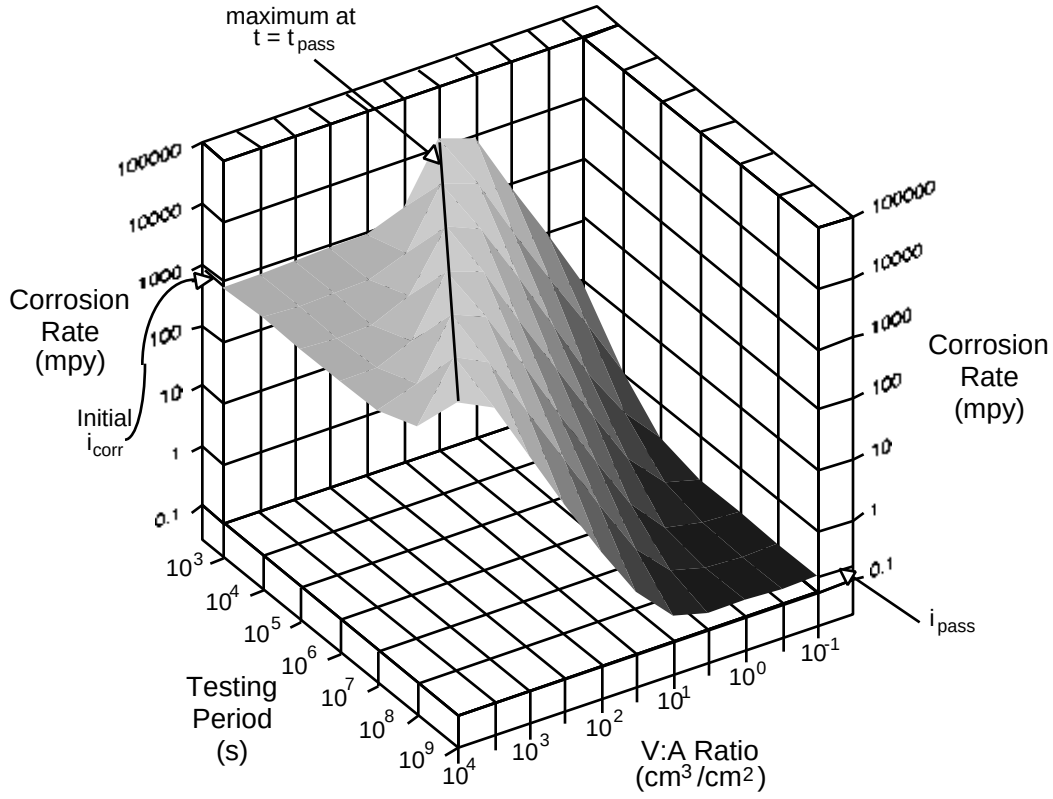

Figure 7 - Plot of calculated corrosion rates that would be obtained from weight loss measurements on 304 SS exposed to 4.1 M HNO_3 + 1 M NaCl as a function of V:A ratio and test period. The calculation assumed that the potential increased linearly with time until passivation. The maximum in corrosion rate occurs when the test period equals the time required for passivation.

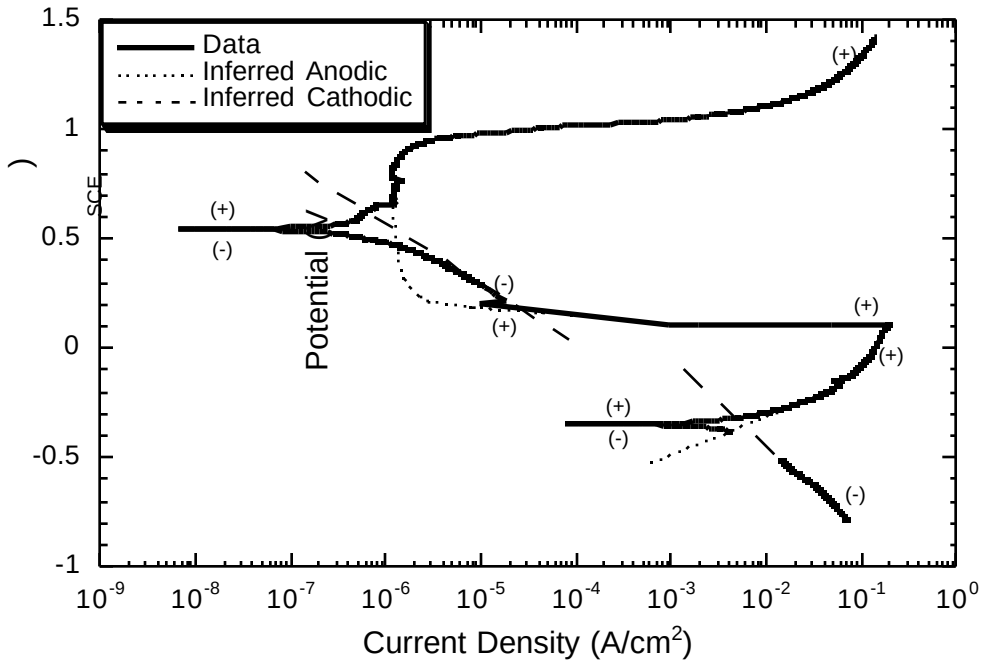

Figure 8 - Graph of anodic and cathodic polarization data from 304 SS immersed in aerated, 22°C, 4.1 M HNO_3 + 1 M NaCl obtained from two separate tests. Dashed lines are inferred anodic and cathodic reactions that are masked by the corresponding opposite reaction. Plus (+) and minus (-) refer to portions of the scan in which the applied current is net anodic and cathodic, respectively. Scans were initiated following 4 hours at OC.

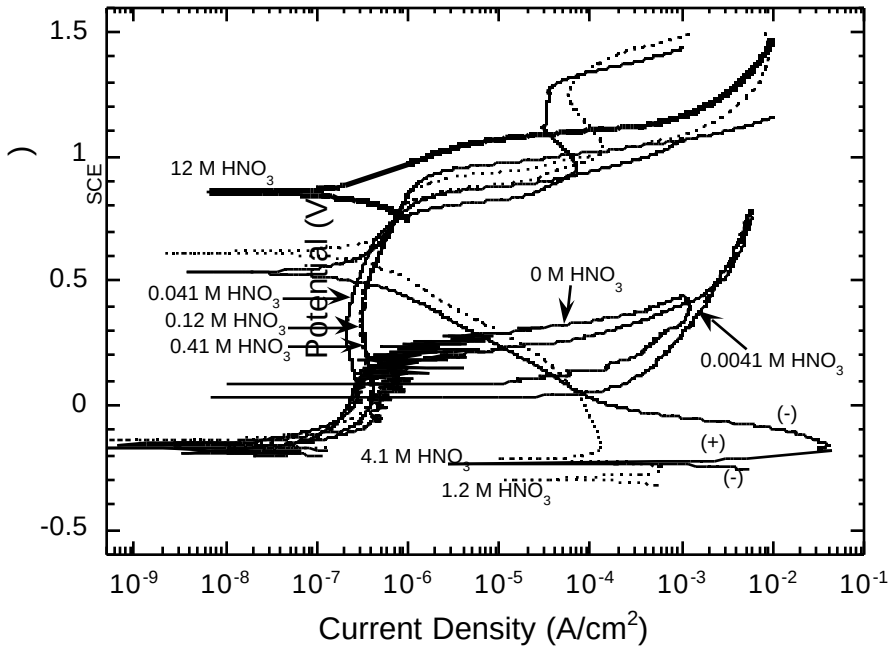

Figure 9 - Potentiodynamic scans composed of 304 SS exposed to aerated, 22°C, 0.3 M NaCl, and varying concentrations of HNO_3. Scans were initiated following 4 hours at OC.

a

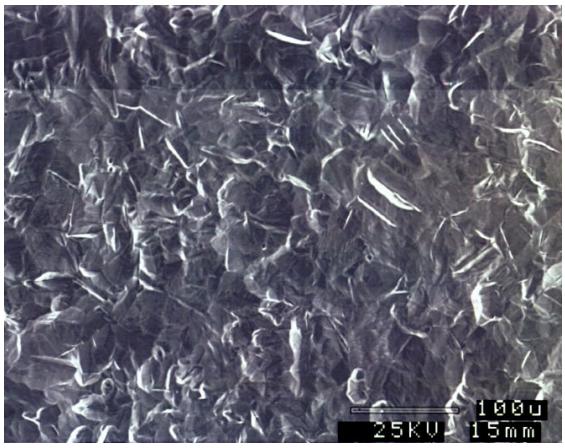

b

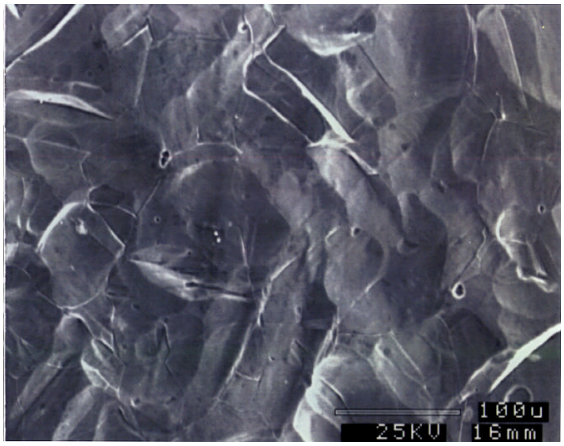

c

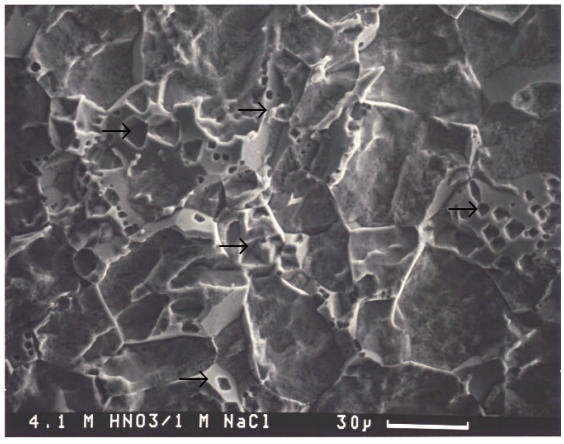

Figure 10 - Micrographs of samples following immersion of 304 SS in aerated, 22°C, 4.1 M HNO_3 + 1 M NaCl: a) preceding passivation (5.6 hour immersion), b) following passivation (24 hour immersion), c) following passivation (168 hour immersion). Examples of faceted grains exhibiting crystallographic pitting are indicated with arrows in c).

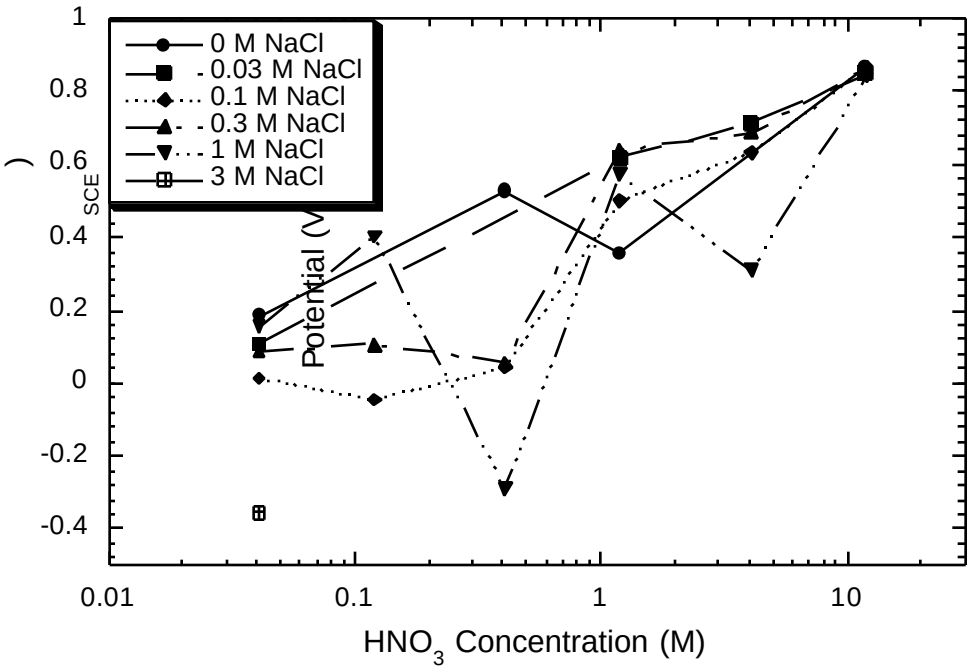

Figure 11 - Measured OCPs of 304 SS at one week. Environments were aerated, 22° C solutions incorporating various concentrations of HNO_3 and NaCl.

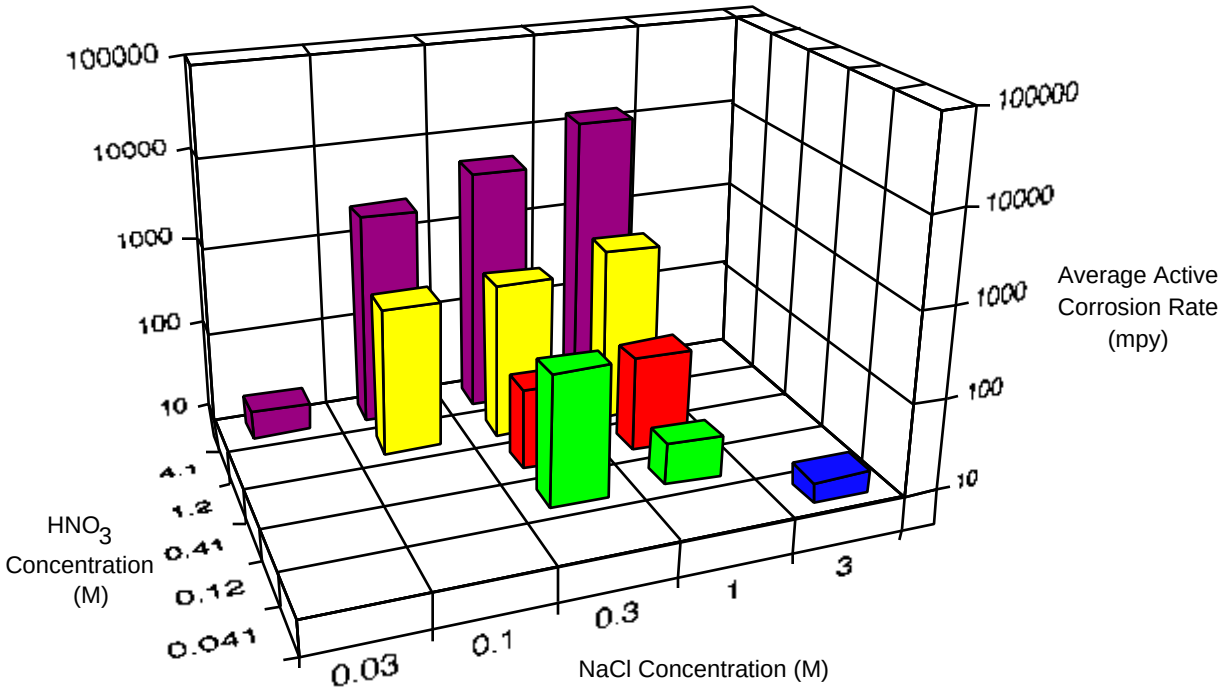

Figure 12 - Plot of average corrosion rate during active corrosion of 304 SS exposed to aerated, 22°C, HNO_3/NaCl environments. These values were obtained by dividing the thickness loss (determined by weight loss measurement) by the time of active corrosion (determined by OCP measurement).

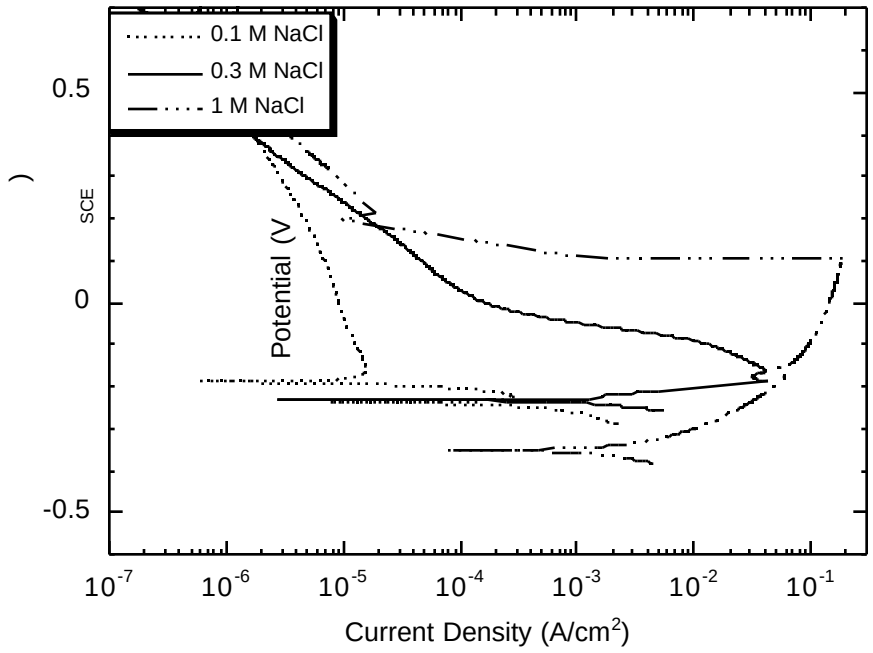

Figure 13 - Potentiodynamic scans on 304 SS exposed to aerated, 22° C, 4.1 M HNO_3 and varying concentrations of NaCl. The 4.1 M HNO_3 + 0.1 M NaCl data were obtained by cathodic polarization following passivation. Scans were initiated following 4 hours at OC. The test incorporating 4.1 M HNO_3 + 1 M NaCl used a 1.0 cm^2 area working electrode to avoid current limitation of the potentiostat and significant ohmic loss in solution.

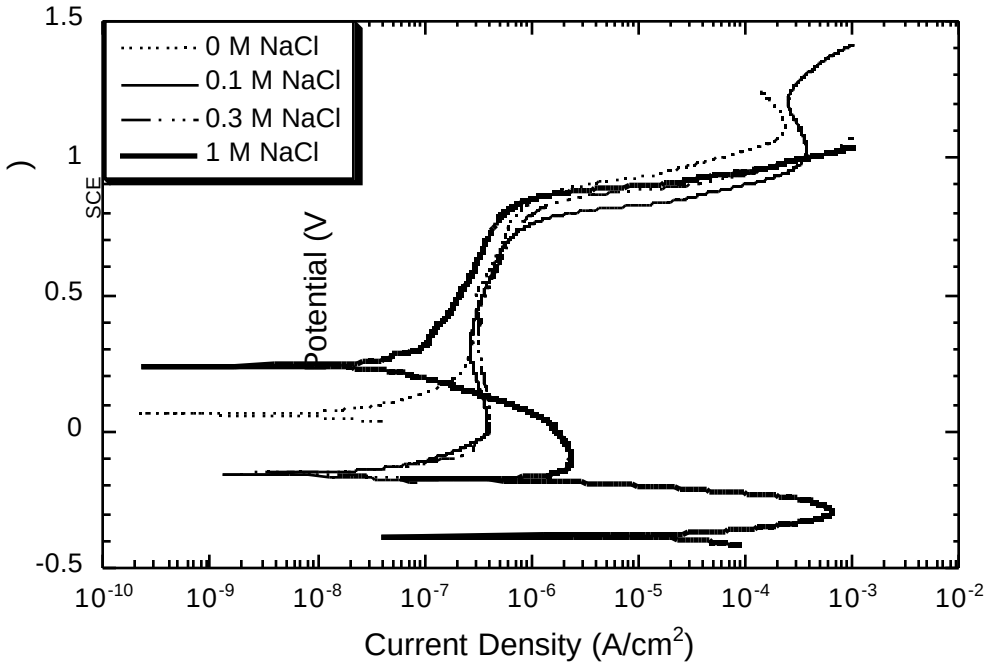

Figure 14 - Potentiodynamic scans comprising 304 SS exposed to aerated, 22°C, 0.41 M HNO_3 and varying concentrations of NaCl. Scans were initiated following 4 hours at OC.

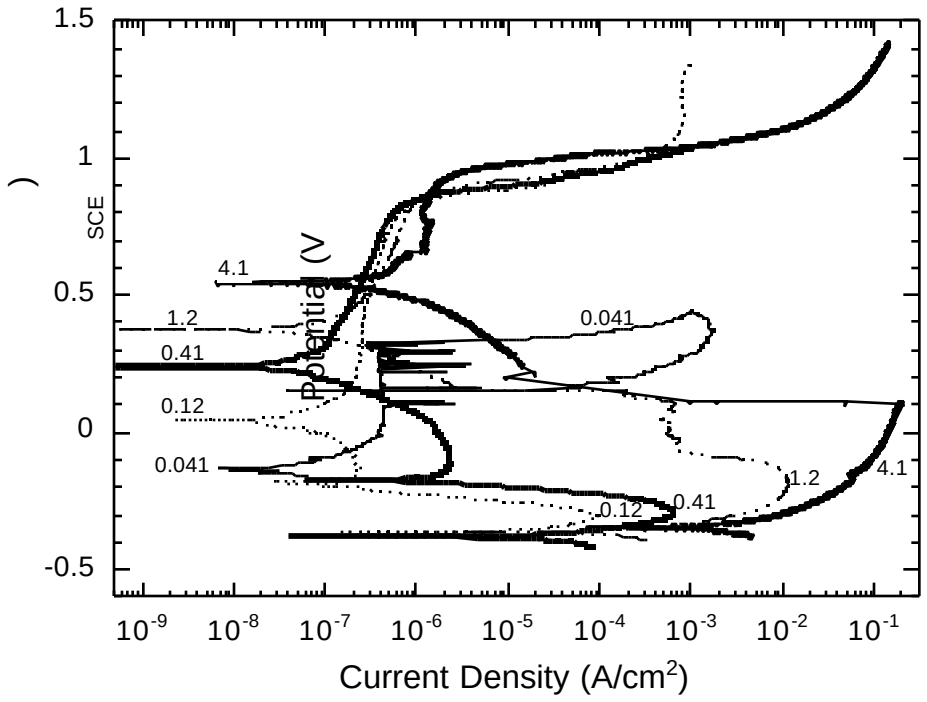

Figure 15 - Potentiodynamic scans composed of 304 SS exposed to aerated, 22°C, 1 M NaCl, and varying concentrations of HNO_3. Scans were initiated following 4 hours at OC. Values represent the concentration (M) of HNO_3 present. Tests incorporating 4.1 M HNO_3 + 1 M NaCl and 1.2 M HNO_3 + 1 M NaCl used 1.0 and 1.6 cm^2 area working electrodes, respectively, in order to avoid current limitation of the potentiostat and significant ohmic loss in solution.

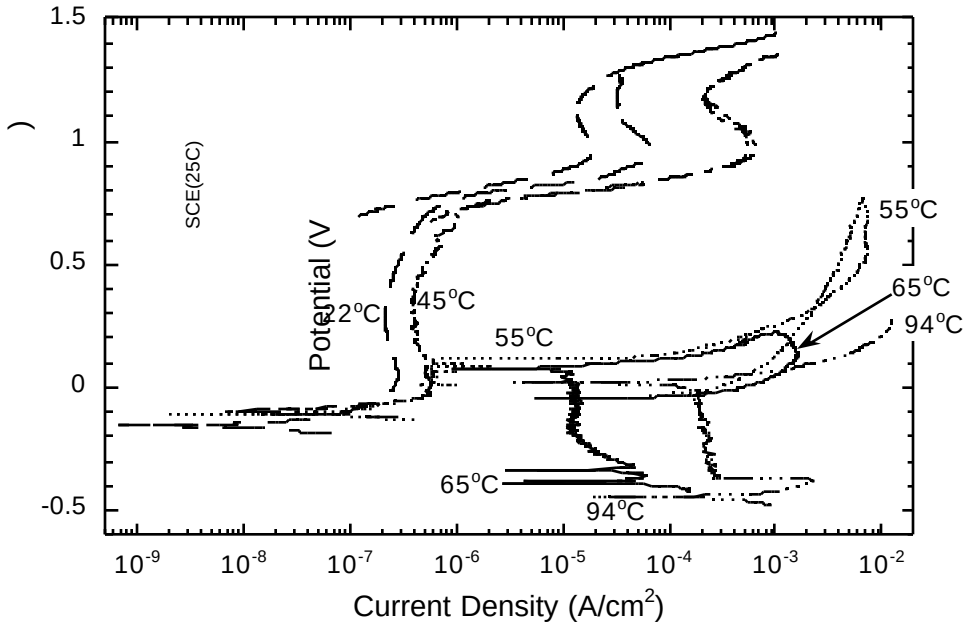

Figure 16 - Potentiodynamic scans composed of 304 SS exposed to aerated, 0.041 M HNO_3 + 0.3 M NaCl at various temperatures. Scans were initiated following 4 hours at OC. All potentials are corrected for temperature and referenced to the SCE at 25°C.

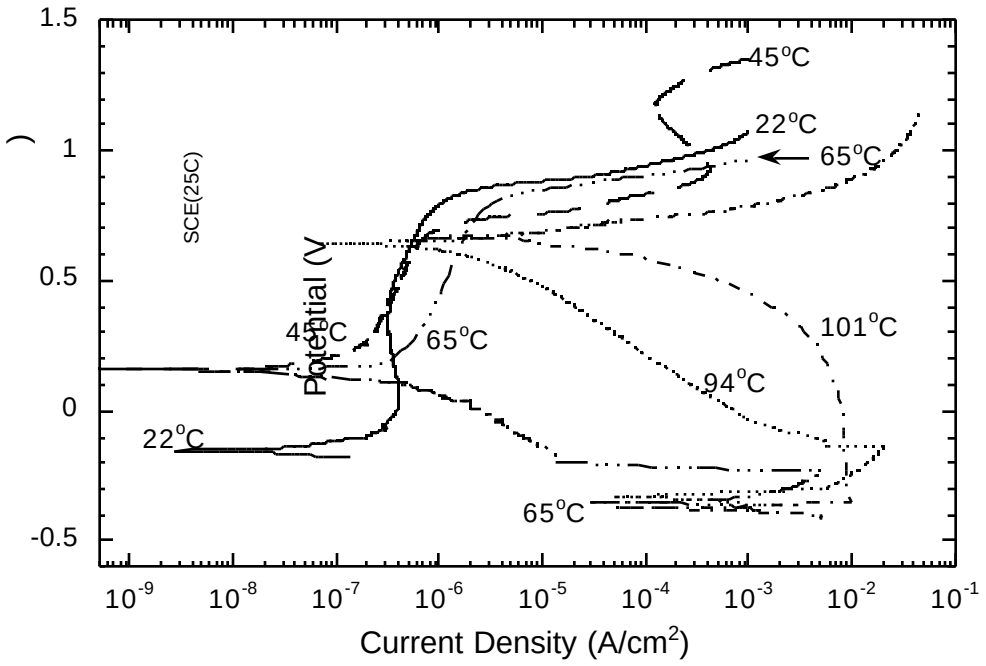

Figure 17 - Potentiodynamic scans composed of 304 SS exposed to aerated, 0.41 M HNO_3 + 0.3 M NaCl at various temperatures. Scans were initiated following 4 hours at OC. All potentials are corrected for temperature and referenced to the SCE at 25°C.

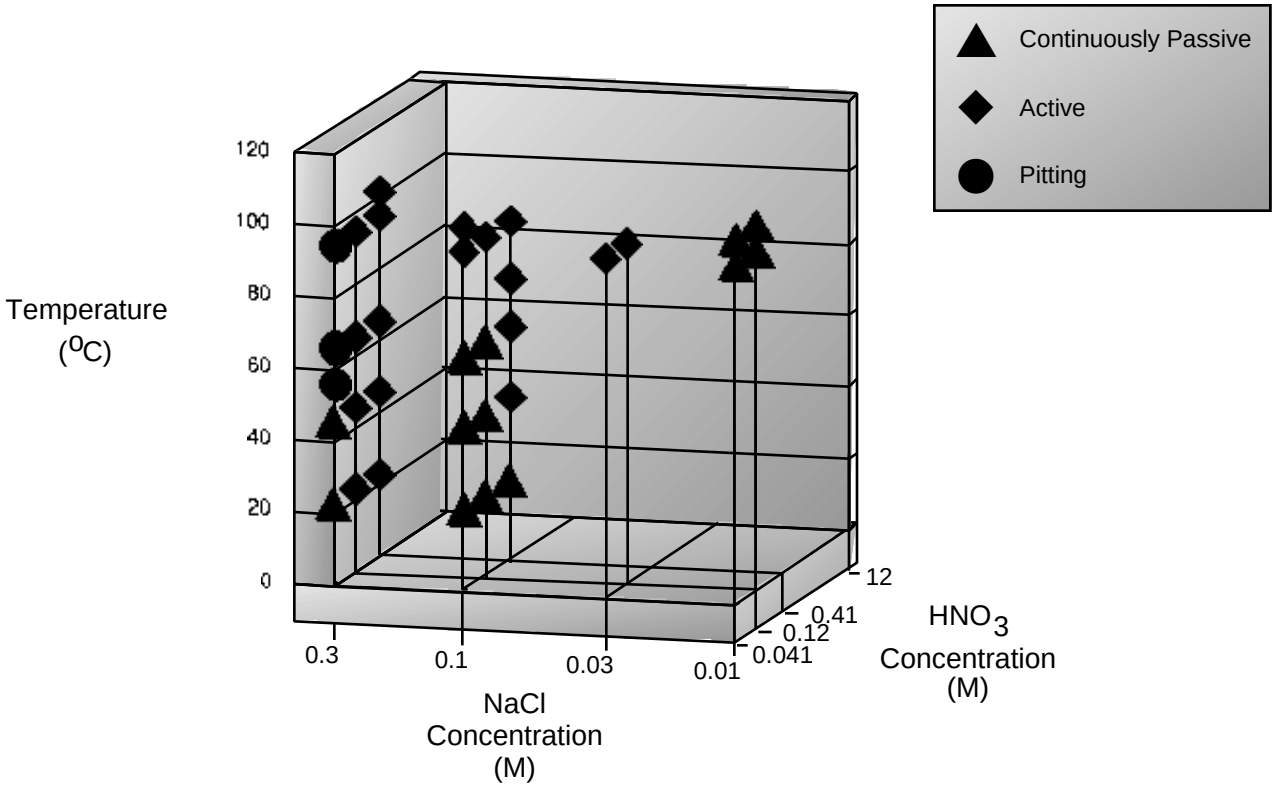

Figure 18 - Plot of corrosion behavior type as a function of HNO_3, NaCl, and temperature (°C). Behaviors were determined from potentiostatic polarization curves following 4 hours at OC. The designation "Active" includes active/passive behavior.